REPORT DOCUMENTATION PAGE

Form Approved
OMB No. 0704-0188

1. REPORT DATE (DD-MM-YYYY)	2. REPORT TYPE	3. DATES COVERED (From - To)
31-07-2003	Technical Paper	

4. TITLE AND SUBTITLE

Comparison of Force Balance Calibration Techniques for the Nano-Newton Range

5a. CONTRACT NUMBER

5b. GRANT NUMBER

5c. PROGRAM ELEMENT NUMBER

6. AUTHOR(S)

Nathaniel P. Selden (USC); Andrew D. Ketsdever (AFRL/PRSA)

5d. PROJECT NUMBER
2308

5e. TASK NUMBER
M19B

5f. WORK UNIT NUMBER

7. PERFORMING ORGANIZATION NAME(S) AND ADDRESS(ES)

Air Force Research Laboratory (AFMC)
AFRL/PRS
5 Pollux Drive
Edwards AFB CA 93524-7048

8. PERFORMING ORGANIZATION REPORT NUMBER

AFRL-PR-ED-TP-2003-199

9. SPONSORING / MONITORING AGENCY NAME(S) AND ADDRESS(ES)

Air Force Research Laboratory (AFMC)
AFRL/PRS
5 Pollux Drive
Edwards AFB CA 93524-7048

10. SPONSOR/MONITOR'S ACRONYM(S)

11. SPONSOR/MONITOR'S NUMBER(S)
AFRL-PR-ED-TP-2003-199

12. DISTRIBUTION / AVAILABILITY STATEMENT

Approved for public release; distribution unlimited.

13. SUPPLEMENTARY NOTES

For presentation in the journal entitled "Review of Scientific Instruments"

14. ABSTRACT

15. SUBJECT TERMS

16. SECURITY CLASSIFICATION OF:			17. LIMITATION OF ABSTRACT	18. NUMBER OF PAGES	19a. NAME OF RESPONSIBLE PERSON
					Leilani Richardson
a. REPORT	b. ABSTRACT	c. THIS PAGE	A	24	19b. TELEPHONE NUMBER (include area code)
Unclassified	Unclassified	Unclassified			(661) 275-5015

Comparison of force balance calibration techniques for the nano-Newton range

Nathaniel P. Selden
University of Southern California, Department of Mechanical and Aerospace Engineering, Los Angeles, California 90089-1191

Andrew D. Ketsdever
Air Force Research Laboratory, Propulsion Directorate, Edwards AFB, California 93524

(Received

With the rapid progress of micro- and nano-scale fabrication technology, devices are continually being created which produce extremely small forces. This creates a distinct need for a measurement instrument and adequate calibration techniques which can resolve forces below 1μN. Two calibration methods for force balance measurements in the nano-Newton range are presented. These methods are based on a free molecule, gas dynamic expansion through a thin-walled orifice and the electrostatic actuation of a miniature comb drive. Due to the advantages and disadvantages of every calibration technique, multiple techniques are often required to validate performance results for micro-scale devices. Because these calibration techniques typically rely on completely different physical processes and can be described by different sets of analytical equations, the comparison of one technique to another is necessary when high accuracy is required. The gas dynamic and electrostatic force calibration techniques have been compared and were found to agree to within 8% for force levels between 35 nano-Newtons and 1μN.

I. INTRODUCTION

The development and performance evaluation of micro- and nano-scale devices has driven the need to measure and accurately resolve force levels below 1 μN. Force measurements with resolution in the nano-Newton range are particularly important for a new generation of micropropulsion systems for small satellite missions.[1] In addition to the development of highly sensitive force balances, a necessary factor for extremely low force measurements is an ability to accurately calibrate the balance's deflection versus a known input force. For example, the Laser Interferometer Space Antenna (LISA) mission currently being planned by NASA requires a micropropulsion system capable of producing thrust levels as low as 1 μN with 0.1 μN resolution.[2] Determining the performance of the LISA propulsion system would, therefore, require a force balance that is accurately calibrated in the ten nano-Newton range.

Conventional methods of calibration, such as hanging weights from a string-pulley system, have been developed for relatively large force measurements (greater than 100 μN) on thrust stands.[3,4] Typically small errors in the milli-Newton force range associated with the weight-hanging calibration technique, such as stiction and the measurement accuracy of the weight-string system mass, become increasingly important in the nano-Newton force range. These previously developed calibration schemes have not proven adequate in providing the level of accuracy required to validate the performance of many micropropulsion systems. Therefore, a new array of calibration techniques have been recently developed by Jamison et al.[5] and Gamero-Castaño et al.[6] for torsion-type thrust stands. These techniques might also be applicable to a wider variety of force

measurement systems. Because different calibration techniques can rely on completely different physical processes and can be described by different sets of analytical equations, the comparison of one technique to another is necessary when high accuracy is required.

As the two most promising calibration techniques developed to date for the nano-Newton force range, the gas dynamic calibration technique of Jamison, et al.[5] and a variation of the electrostatic calibration technique of Gamero-Castaño et al.[6] are compared in this manuscript. Both calibration schemes have advantages and disadvantages. The advantages of both techniques include the simplicity of implementation and use, the ability to perform in-situ calibration, and the means to accurately determine the applied forces through validated analytical equations. The additional advantage of the gas dynamic technique is the ability to calibrate the force balance in the same manner as the micro-scale device produces force (for devices which utilize gaseous flows), and the additional advantage of the electrostatic calibration technique is the ability to easily calibrate both steady-state and impulse measurements.

II. GAS DYNAMIC FORCE CALIBRATION

The gas dynamic (GD) calibration technique relies on the free molecule (FM) expansion of a gas through a thin-walled sonic orifice.[5] FM flow is defined as a flow in which the distance traveled, on average, by a gas molecule is much larger than the characteristic dimension of the flow. The FM flow condition is used in the GD technique for two reasons. First, the GD technique produces force levels in the nano-Newton range for reasonably sized orifices at measurable operating pressures; second, well defined

analytical solutions exist for the mass flow and force (and thus, propulsive specific impulse) produced by FM flows. However, the FM flow limit implies that the GD technique is only useful for force balances contained in a vacuum system – one of the technique's disadvantages.

For free molecule flow, the force from an orifice is given by

$$F_{GD} = \frac{p_O}{2}\left(1 - \frac{2t}{d}\right)A \tag{1}$$

where p_o is the orifice stagnation pressure, t is the orifice thickness, d is the orifice diameter, and A is the orifice area. Equation (1) has been validated for thin-walled (i.e., t/d « 1) orifice flow by experimental[5] and numerical[7] investigation of high Knudsen number orifice flows.

The implementation of the GD calibration system on the thrust stand used in this study is shown schematically in Fig. 1. The orifice was conventionally machined in a tantalum shim with a diameter of 1mm ±0.025mm with a wall thickness of 0.015mm giving a t/d=0.015. The orifice was attached to an aluminum plenum with much greater internal dimensions than the orifice, which allowed for a uniform flow condition in the plenum.

III. ELECTROSTATIC FORCE CALIBRATION

Gamero-Castaño et al.[6] discussed an electrostatic (ES) calibration technique which utilized two parallel electrodes separated by a gap. The force produced by the parallel electrode ES technique is given by

$$F_{ES,P} = \frac{1}{2}\varepsilon_o\left(\frac{V}{L}\right)^2 A_p \tag{2}$$

where ε_o is the permittivity of the gap medium, V is the voltage difference applied to the parallel electrodes, L is the gap separation distance, and A_p is the area of the electrodes. As Eq. (2) indicates, the force is inversely dependent on the square of the gap distance. For torsion thrust stand applications where only one electrode is attached to the stand, the electrode spacing will change during the operation of the calibration system. Because of the $1/L^2$ dependence, even a small change in L can lead to relatively large errors in the assumed calibration force. Due to this limitation of the parallel electrode ES technique, a new calibration technique based on ES combs (ESC) was designed for the purposes of this work.

A specialized version of the comb ES actuator described by Johnson and Warne[8] was fabricated for the purposes of ES calibration of a force balance. A schematic with the geometry of a single comb assembly is shown in Fig. 2. The force produced by the engaged combs for a comb width equal to the separation gap between the combs (i.e., c=g, see Fig. 2) is given by

$$F_{ES,C} = 2N\varepsilon_o V^2\left(1.0245 - \frac{g}{\pi x_o}\right) \tag{3}$$

where N is the number of comb pairs, and g and x_o are defined in Fig. 2. Equation (3) is valid for infinitely combs when the ratio $x_o/g > 1.5$. For large values of x_o/g, the force asymptotes near $2N\varepsilon_o V^2$. Therefore, the benefits of the ESC technique for torsion thrust stands can be seen in Eq. (3) where the force can be relatively independent over a

reasonable range of the comb engagement distances, x_o. The applicability of Eq. (3) for ESC calibration was validated experimentally in this study.

IV. EXPERIMENTAL SETUP AND PROCEDURE

The GD and ESC calibration systems were mounted on the nano-Newton Thrust Stand (nNTS) which has been described in detail elsewhere.[5] The unique feature of the nNTS for this study was its ability to accurately measure steady-state forces as low as 34 nN ± 9%. The level of accuracy of the nNTS was important for the comparison data in order to measure the small differences expected between the calibration techniques. The GD orifice and the ES combs were arranged on an aluminum plenum (attached to the nNTS) as shown in Fig. 3. The position of force generation for both techniques was the same distance from the nNTS center of rotation. The nNTS was installed in a 3m diameter by 6m long high vacuum chamber that maintained background pressures below 10^{-5} Torr for all of the tests in this study.

The GD calibration system was operated on helium with a stagnation temperature of 297 K, and the orifice stagnation pressure was measured using a standard pressure transducer. The pressure transducer used in this work had a minimum resolution of 0.1 mTorr. The helium was introduced into the orifice plenum through the nNTS inverted cylinder geometry which allowed for thrust stand operation without the direct coupling between the thrust stand and the gas feed line as shown in Fig. 1.[5] This helped to insure that any differences between the two techniques did not come from differences in the calibration system infrastructure.

The ES comb calibration system was mounted on the nNTS such that the grounded portion of the combs was physically attached to the thrust stand, which was also grounded to the vacuum facility. This was done so that there was no need to couple wires to any part of the nNTS. The ECS system set up on the nNTS is shown in Fig. 4. The part of the comb system not directly attached to the nNTS was supplied with a voltage through a high voltage power supply outside the vacuum chamber. The power supply output was verified to be stable to within 0.5% over the length of a typical steady-state force calibration. The ESC system was aligned using a three-dimensional micrometer stage on which the powered comb section was attached. The combs were nominally placed with an engagement distance at 5.0mm. The engagement distance was accurately measured for each experiment by a linear micrometer.

Verification data was taken with the ECS calibration system on a mass balance in a configuration shown in Fig. 5. One-half of the ECS system was placed vertically on the mass balance with a grounding wire attached to the pallet. The variable potential comb assembly was placed above it on a three-axis positioning stage. Accurate alignment and measurement of the comb engagement distance was accomplished through the use of the micrometer positioning stage. The mass balance used for this work had a resolution of $5x10^{-6}$g.

V. RESULTS

Figure 6 shows experimental results of normalized force versus x_o/g for the ESC calibration system developed in this study. Two theoretical lines have also been added to Fig. 6. The first theoretical line shows the approximation for infinite combs from Eq. (3). The second combines Eq. (2) and Eq. (3) in an attempt to account for the finite comb length of the ECS configuration of this study, where it was assumed that the comb ends of one-half and the back portion of the other half of the comb configuration produce a parallel plate capacitance between the two sections. Figure 6 shows departure from the ideal infinite comb analytical solution for $x_o/g < 1.5$ and for $x_o/g > 6$. At $x_o/g > 6$, the three-dimensional behavior of the ESC system is apparent. The departure from the analytical solution in Eq. (3) is most likely due to the capacitance between the straight-walled sections of the combs which increases with engagement distance, fringing effects, and other three-dimensional effects. Although the trend in the normalized force versus x_o/g data is consistent with the combined comb/parallel plate equations, the absolute value is not captured, indicating other effects may contribute to the force generated by the ECS system for $x_o/g > 6$. Good agreement between the experimental data and Eq. (3) is shown for engagement distances between 2 and 5mm. Figure 7 shows the ESC force as a function of applied voltage for $x_o = 4.0$, 5.0, and 6.0mm. The data in Fig. 7 indicates that a change in the ESC engagement distance of 1mm will lead to a 2% change in the force produced assuming a nominal engagement of 5.0mm. Since the engagement distance can be verified to within 0.1 mm even inside the vacuum facility, the error associated with the ESC engagement distance will not lead to major errors in the predicted performance derived from the calibration system. A nominal engagement distance of 5.0mm was used throughout the rest of this study.

The behavior of the ESC calibration system on the nNTS was validated by comparing the thrust stand deflection as a function of applied voltage to the normalized deflection of the mass balanced. The comparison is shown in Fig. 8. The mass balance data was taken at atmospheric conditions while the thrust stand data was obtained in vacuum, and the slight differences in the permittivity of the intervening media has been taken into consideration. Both the nNTS and mass balance data agree to within 3% of the ESC theory in Eq. (3), indicating that the ESC system was physically behaving as predicted. The combination of the mass balance and the nNTS experimental data was used to validate the accuracy of the analytical ES theory of Eq. (3).

Figure 9 shows the results of the nNTS deflection as a function of the GD calibration system stagnation pressure. The force associated with the stagnation pressure was derived from Eq. (1), which was verified numerically in previous work.[7] The Knudsen number for the helium GD calibration system flow ranged from approximately 10 to 180 over the range of stagnation pressures shown in Fig. 9. The calibration line is the best fit linear interpolation of the data points. The vertical error bars represent the standard deviation in the data repeatability for at least five different tests at the same stagnation pressure. The standard deviations are less than 4.5% at the lowest pressures, but improve to less than 1% at the higher end of the pressure range investigated. The horizontal error bars represent the error in the pressure measurements in the orifice plenum due to the minimum resolution of the pressure transducers used.

Figure 10 shows the comparison of the GD and ESC calibration techniques obtained on the nNTS over the force range from 104 nN to 1.2 μN. The forces indicated were derived from the validated equations Eq. (1) and Eq. (3) for the GD and ESC systems respectively. The results of the calibration system comparison were promising, with the slopes of the GD and ECS data sets falling to within 8%. It is expected that the two calibration techniques would not agree well at force levels above 1 μN due to the fact that the GD technique is transitioning from a FM condition, where Eq. (1) is valid, to a less rarefied flow regime, where Eq. (1) begins to lose its applicability. The force calculated by Eq. (1) will be lower than the actual force produced for forces above 1 μN (corresponding to orifice stagnation pressures above 14.3 mTorr). This limitation is only a function of the GD system design for this study (i.e., based on the orifice diameter and operational pressure range chosen) and not a limitation of the overall GD technique.

VI. DISCUSSION

The need for new calibration techniques for thrust stands (and force balances, in general) has been highlighted for the nano-Newton force range. Because of the advantages and disadvantages of individual techniques, it is evident that several different calibration techniques will be needed to address different aspects of research. For example, the major disadvantage of the GD system is the necessity of a vacuum expansion. In cases where vacuum is not convenient for a given force balance arrangement, the ESC technique can be used. However, the major advantage of the GD system is the ability to calibrate a thrust stand in the same manner as the force is being produced by a device operating on gas flow (such as a micro-thruster assembly), which brings to light a major

limitation of the ESC system. As such, the comparison of the GD and ESC calibration techniques to within 8% has been a key factor in validating both techniques for use in the nano-Newton force range.

The largest contribution to the variation in the two techniques is most likely the error associated with the GD pressure measurements. Although the pressure transducers used in this study were carefully calibrated, systematic sensor errors, absolute calibration errors, and errors associated with the minimum resolution of the pressure sensors could not be completely negated. However, comparison of two completely different techniques based on different physical processes to this level of agreement is considered important. Not only have the techniques been validated, but the analytical solutions for the force generated as a function of basic parameters have also been experimentally validated for both the GD and ESC techniques investigated in this study.

An improved version of the ES calibration system described by Gamero-Castaño et al.[6] has been developed for the purposes of calibrating torsion force balances. The unknowns in position of a torsion balance can lead to large errors in determining the force produced by parallel plate electrodes by analytical means. For example, the error associated with an unknown on the order of 10μm in the distance of a 1mm gap is approximately 2%. This error can be dramatically reduced by the use of ES comb actuation. For example, the unknown can be on the order of 1 mm in an engagement distance of 5mm for the same 2% error. For force balances contained inside vacuum chambers, position errors on the order of tens of micrometers can be expected due to thermal drift, pump down

processes, and other factors. For many systems, in-situ diagnostics of gap distances may not be convenient or even possible; therefore, the use of the ES comb calibration system has obvious benefits over the parallel plate versions described in other work.[6]

For the calibration of larger force measurements, the continuum flow regime, which also has analytical force solutions, can be explored for the GD calibration technique. The GD technique can be pushed into the continuum flow regime by increasing the orifice diameter and/or increasing the orifice stagnation pressure. Extension of the GD technique to the mN to N range would be straightforward but would require validation of the continuum solutions for the particular calibration system configuration.

Acknowledgments

The authors acknowledge Prof. E.P. Muntz for his assistance and suggestions. This work was supported by the Air Force Research Laboratory, Propulsion Directorate, Space and Missile Propulsion Division (AFRL/PRSA), Edwards AFB, California.

REFERENCES

1. J. Mueller, *Micropropulsion for Small Spacecraft, Progress in Astronautics and Aeronautics*, edited by M. Micci and A. Ketsdever (AIAA, Reston, VA, 2000), Vol. 187, pp. 45-137.

2. W. Willis, C. Zakrzwski, and S. Merkowitz, AIAA Paper No. 2002-3820, July 2002.

3. M. Wilson, S. Bushman, and R. Burton, 25th International Electric Propulsion Conference, IEPC Paper No. 97-122, Cleveland, OH, 24-28 August 1997.

4. J. Lake, G. Cavallaro, G. Spanjers, P. Adkison, and M. Dulligan, AIAA Paper No. 2002-3821, July 2002.

5. A. Jamison, A. Ketsdever, and E.P. Muntz, Rev. Sci. Instrum., **73**, 3629 (2002).

6. M. Gamero-Castaño, V. Hruby, and M. Martinez-Sanchez, 27th International Electric Propulsion Conference, IEPC Paper No. 01-235, Pasadena, CA, 15-19 October 2001.

7. A. Alexeenko, S. Gimelshein, D. Levin, A. Ketsdever, and M. Ivanov, *Proceedings of the 23rd International Symposium on Rarefied Gas Dynamics*, edited by. A. Ketsdever and E.P. Muntz, (AIP, New York, NY, 2003), pp. 565-571.

8. W. Johnson and L. Warne, J. Microelctromechanical Systems, **4**, 49 (1995).

FIGURE CAPTIONS

Figure 1: Typical configuration of the gas dynamic calibration technique on the nano-Newton Thrust Stand.

Figure 2: Schematic of the electrostatic comb calibration system geometry. A: End view, B: Side view. Shaded combs represent those to which voltage is applied and unshaded combs are electrically grounded.

Figure 3: Schematic of gas dynamic calibration system plenum with grounded electrostatic comb section attached.

Figure 4: Close-up view of the installation of the gas dynamic orifice plenum and electrostatic comb assembly on the nano-Newton Thrust Stand.

Figure 5: Schematic of the electrostatic comb calibration system on the mass balance.

Figure 6: Normalized force data from various engagements of the ES combs at a potential difference of 600V. Note: Error bars are less than the symbol size.

Figure 7: Force as a function of applied voltage difference to the ESC system for engagement distances of 4.0, 5.0, and 6.0 mm.

Figure 8: Normalized deflection versus applied ES comb voltage difference for the mass balance and the nNTS. The comparison shows that the two experimental verifications agree with theory to within 1%.

Figure 9: Deflection versus stagnation pressure for the GD calibration system operating on helium in the free molecule flow regime.

Figure 10: Comparison of deflection versus force calibration between the ES comb technique and gas dynamic technique. The slopes of the two lines fall within 8% of one another.

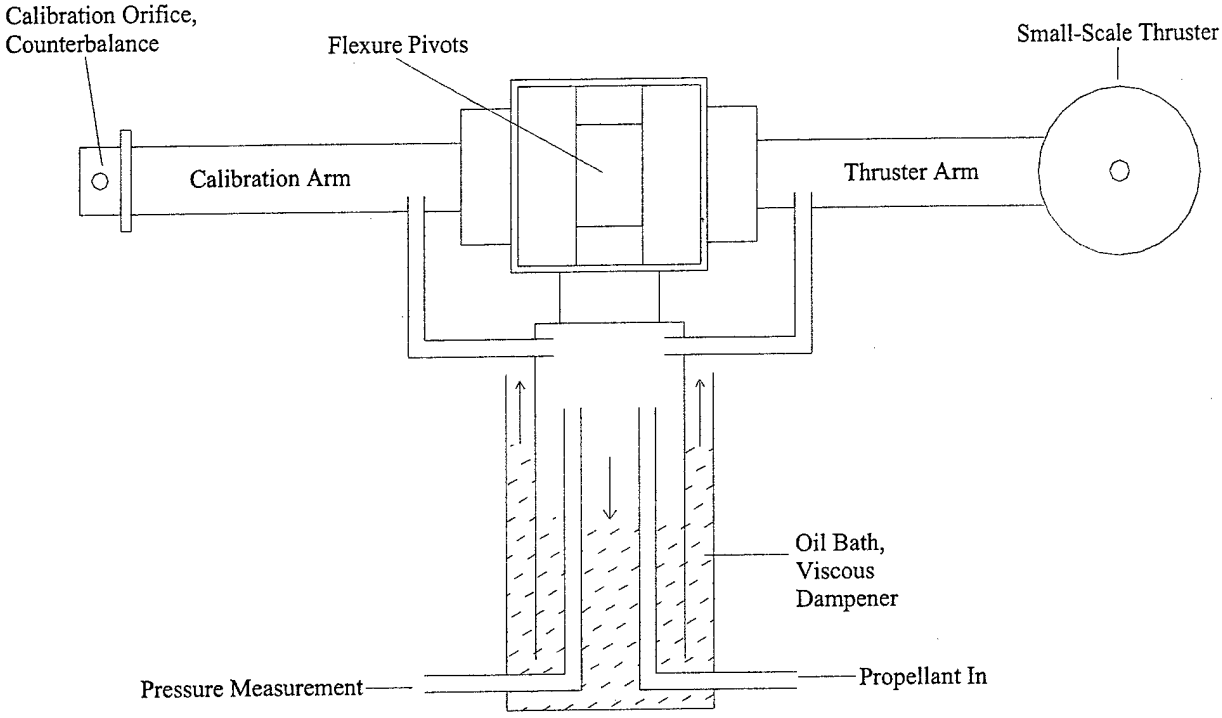
Calibration Orifice,
Counterbalance
Flexure Pivots
Small-Scale Thruster
Calibration Arm
Thruster Arm
Oil Bath,
Viscous
Dampener
Pressure Measurement
Propellant In

Figure 1

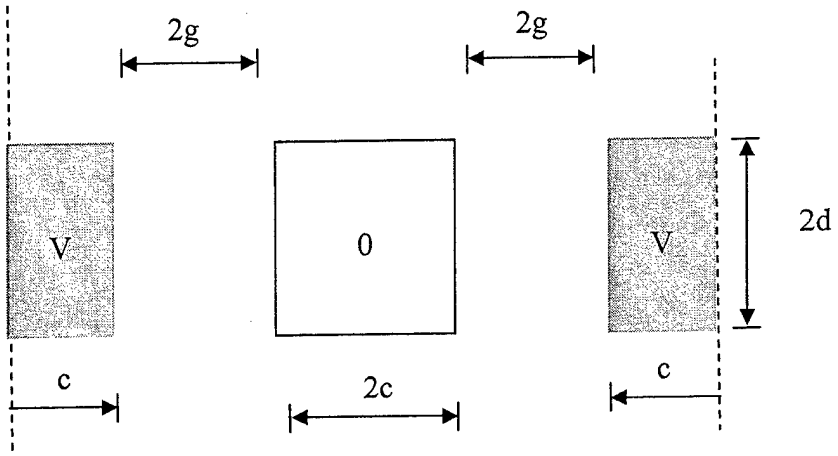

(A)

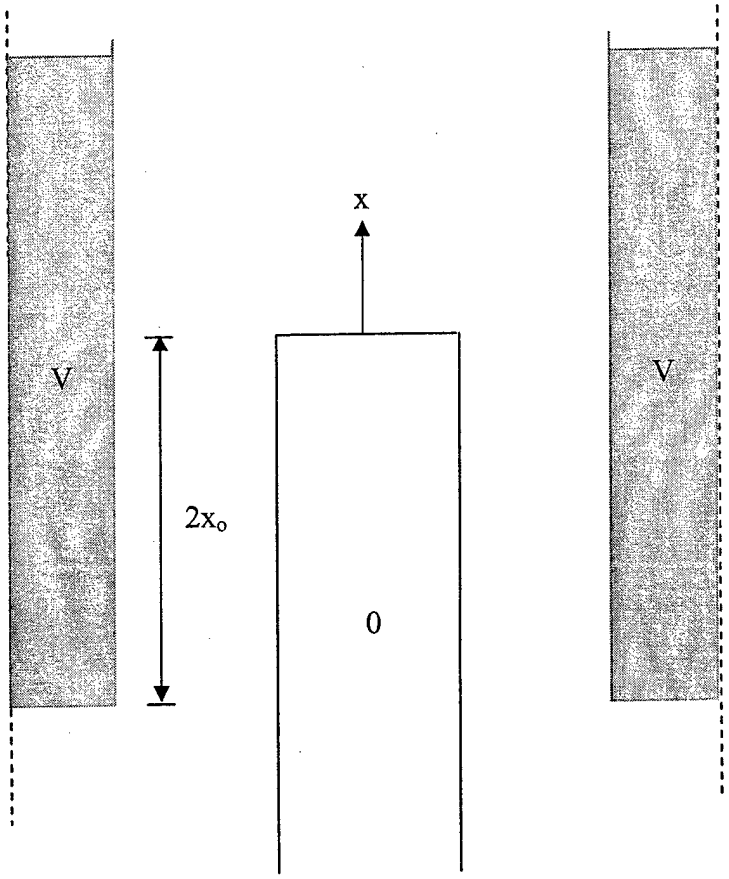

(B)

Figure 2

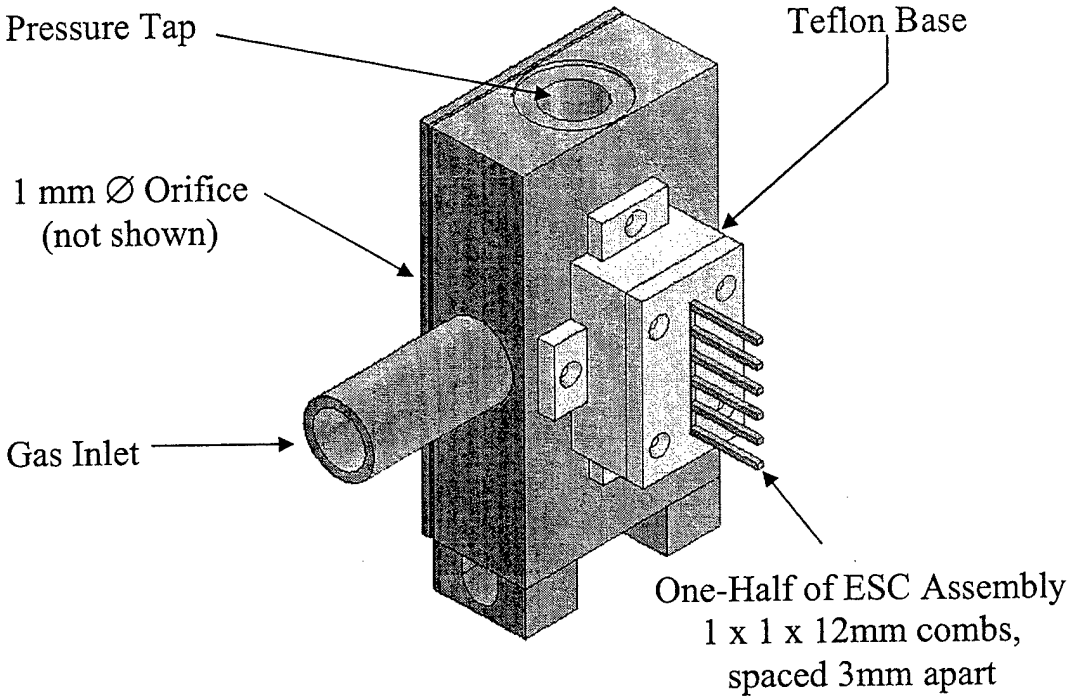
Pressure Tap
Teflon Base
1 mm ∅ Orifice
(not shown)
Gas Inlet
One-Half of ESC Assembly
1 x 1 x 12mm combs,
spaced 3mm apart

Figure 3

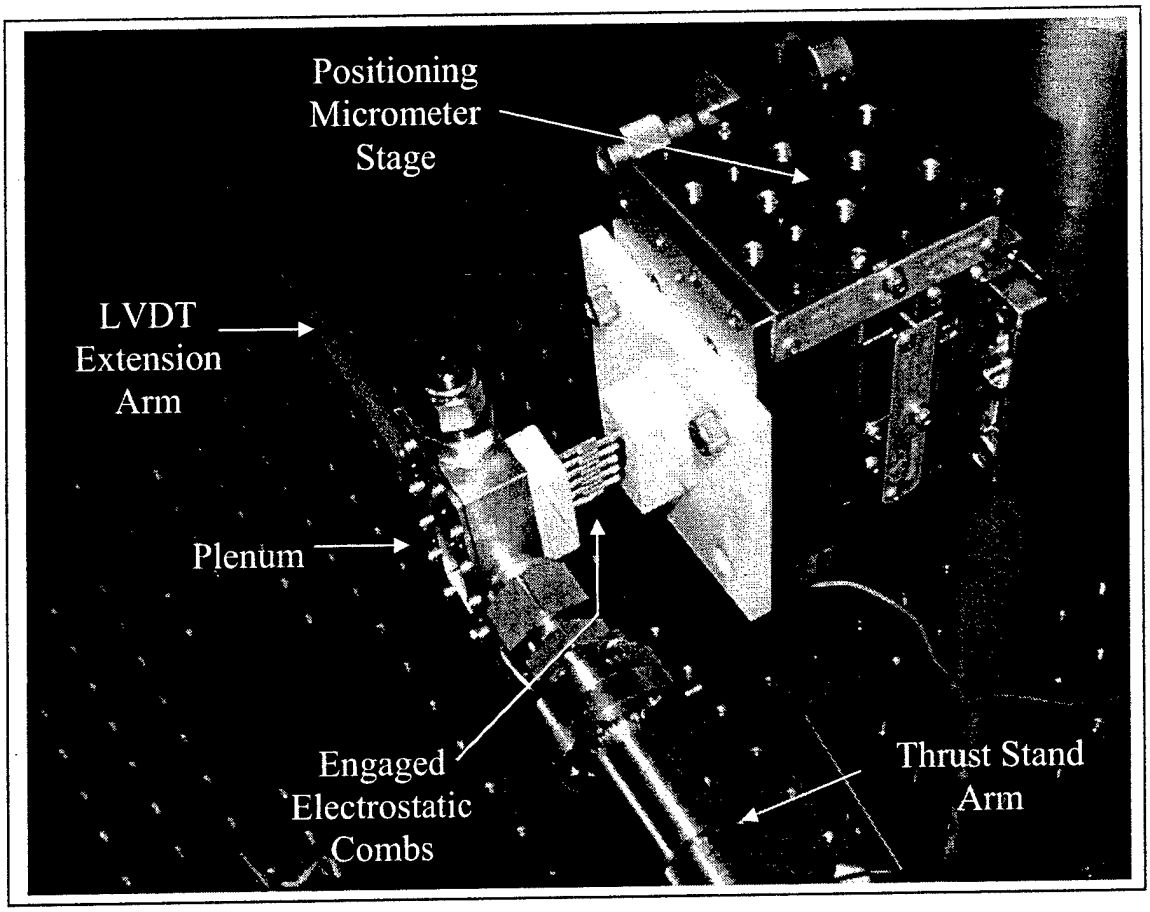
Positioning
Micrometer
Stage
LVDT
Extension
Arm
Plenum
Engaged
Electrostatic
Combs
Thrust Stand
Arm
Figure 4

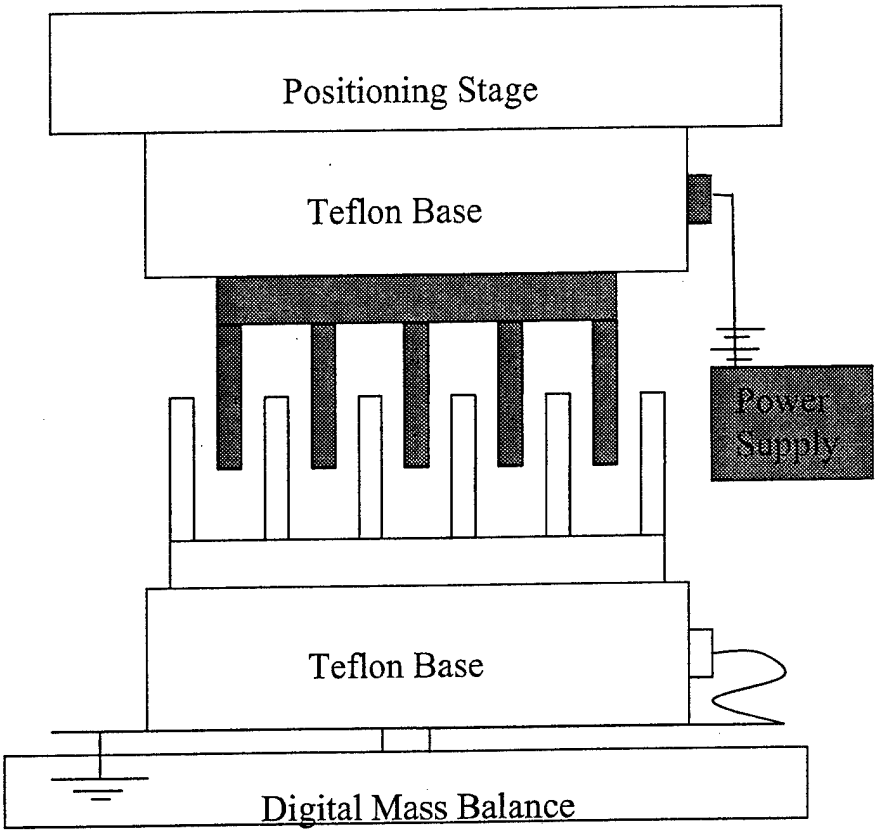
Positioning Stage
Teflon Base
Power Supply
Teflon Base
Digital Mass Balance

Figure 5

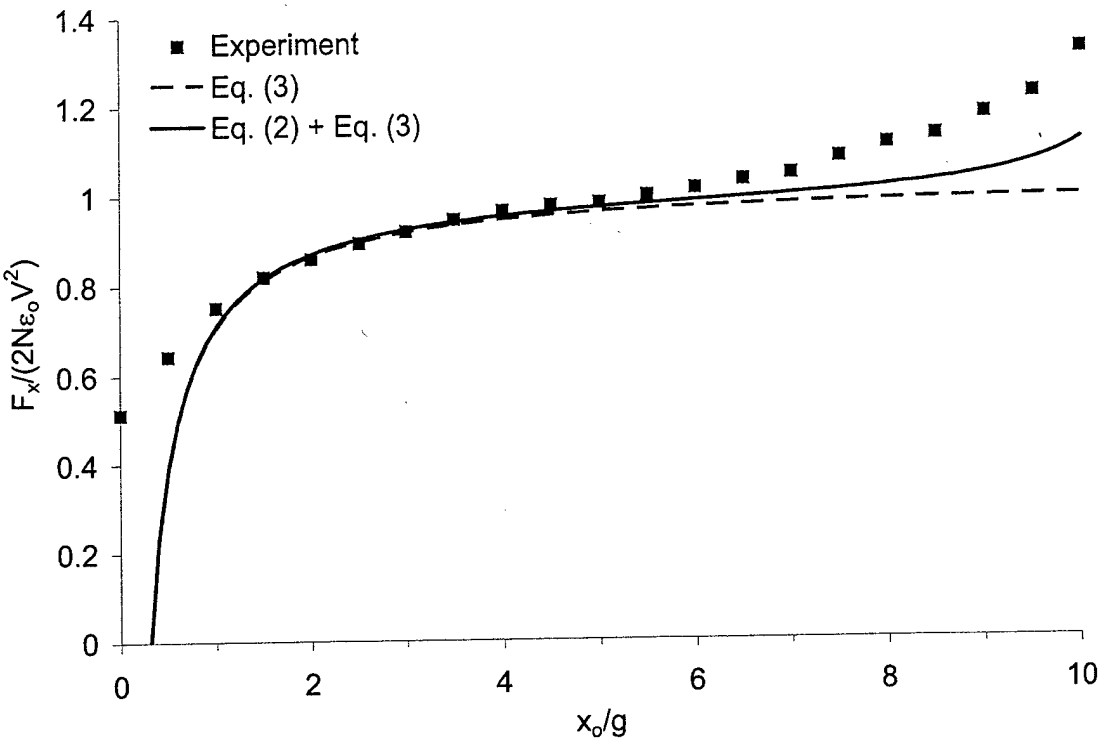
Experiment
Eq. (3)
Eq. (2) + Eq. (3)
1.4
1.2
1
0.8
0.6
0.4
0.2
0
$F_x/(2N\varepsilon_o V^2)$
0
2
4
6
8
10
x_o/g

Figure 6

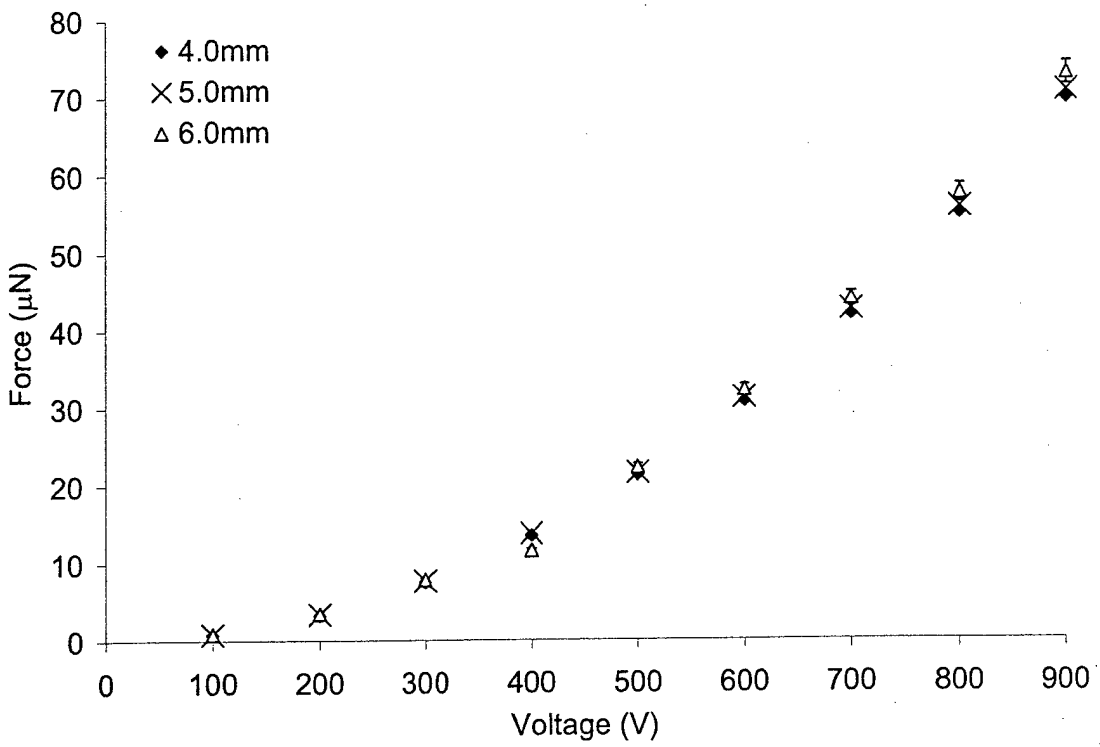
4.0mm
5.0mm
6.0mm
Force (μN)
Voltage (V)
0
10
20
30
40
50
60
70
80
0
100
200
300
400
500
600
700
800
900

Figure 7

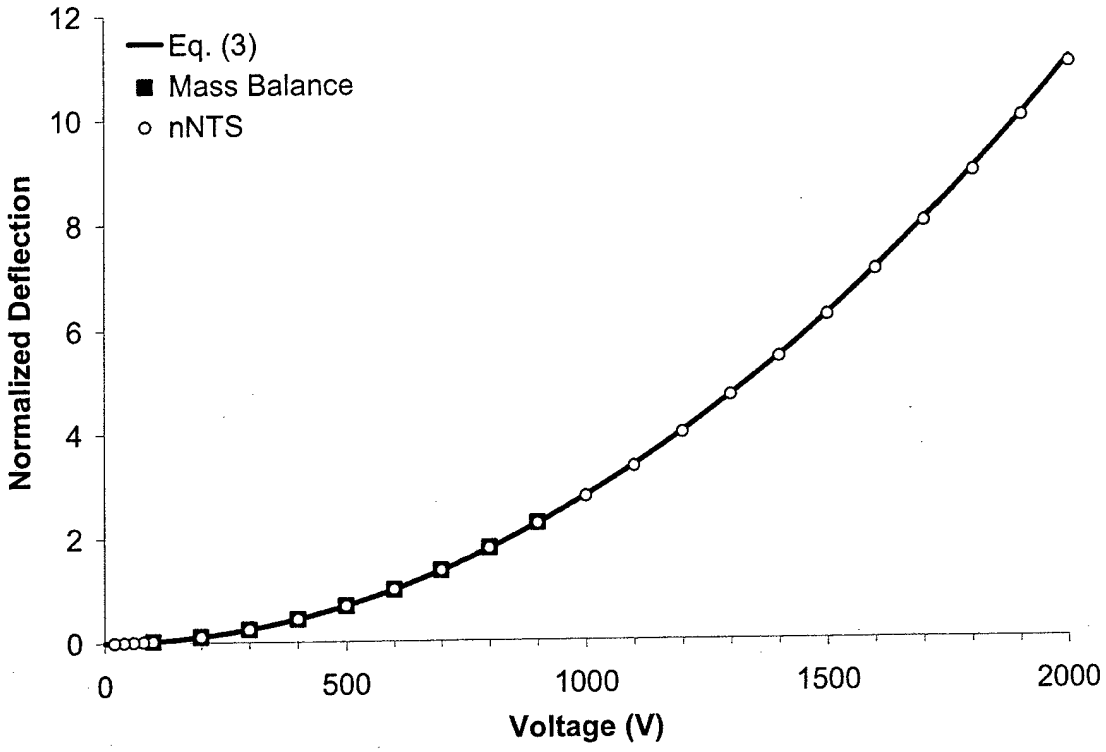
12
10
8
6
4
2
0
Normalized Deflection
Eq. (3)
Mass Balance
nNTS
0
500
1000
1500
2000
Voltage (V)

Figure 8

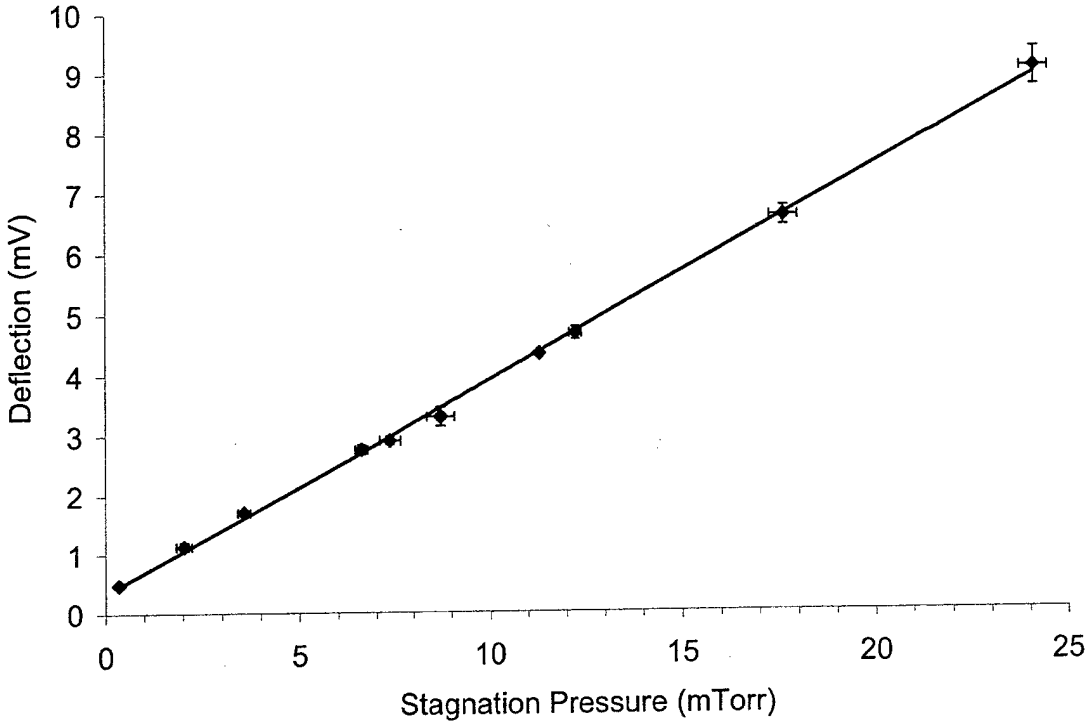
Deflection (mV)
10
9
8
7
6
5
4
3
2
1
0
0
5
10
15
20
25
Stagnation Pressure (mTorr)

Figure 9

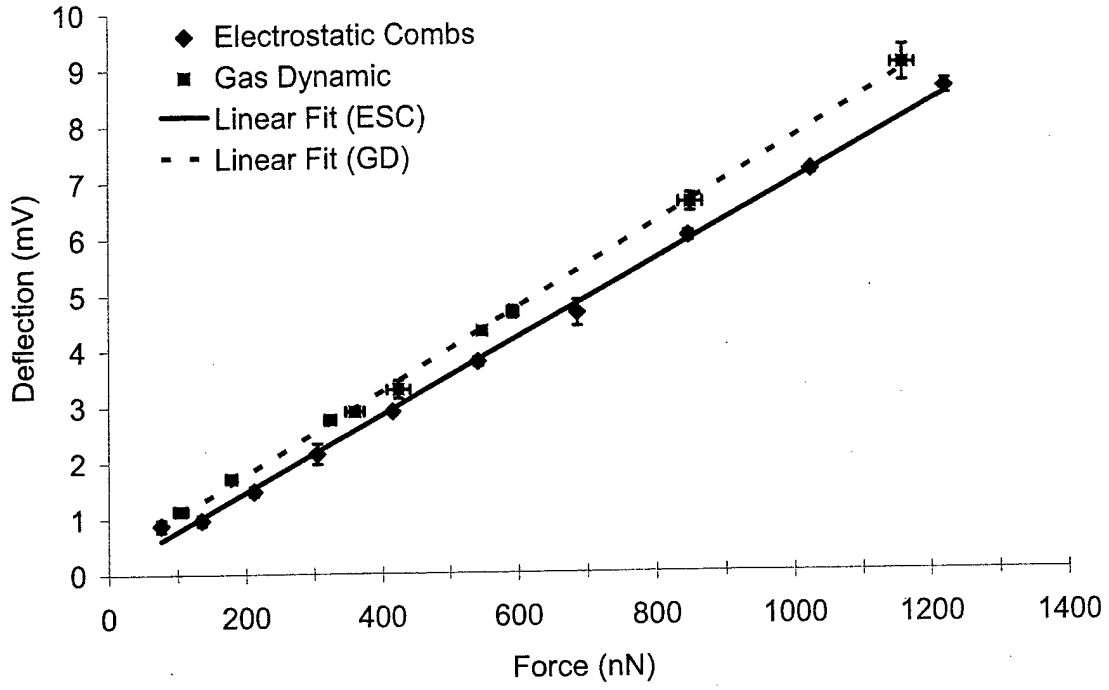
Electrostatic Combs
Gas Dynamic
Linear Fit (ESC)
Linear Fit (GD)
Deflection (mV)
Force (nN)
0
1
2
3
4
5
6
7
8
9
10
0
200
400
600
800
1000
1200
1400

Figure 10